ELSEVIER

Environmental Modelling & Software 16 (2001) 481–493

Environmental Modelling & Software

www.elsevier.com/locate/envsoft

A semi-distributed approach to rainfall-runoff modelling—a case study in a snow affected catchment

Teemu Kokkonen *, Harri Koivusalo, Tuomo Karvonen

Laboratory of Water Resources, Helsinki University of Technology, P.O.Box 5200, FIN-02015 HUT, Finland

Received 21 September 2000; received in revised form 6 December 2000; accepted 16 February 2001

Abstract

A semi-distributed hydrological model was applied to a small forested catcment in southern Finland. The aim was to demonstrate how differences in terrain properties could be taken into account in modelling runoff generation, and to test how well the presented model simulated streamflow with only limited calibration. Modelling was based on subdivision of a catchment into topographically similar areas, which were identified from a digital elevation model. The water balance in each area was calculated using a hillslope-scale model. Discharges from the set of hillsope-scale models were combined with the aid of a routing procedure to yield the total streamflow at the catchment outlet. The catchment receives approximately 30% of the annual precipitation as snow, and thus a snow model was required in winter periods. The presented semi-distributed model was capable of reproducing fairly well the measured streamflow when only two model parameters were calibrated against streamflow. The results suggested that unlike the cumulative runoff, the temporal variability of runoff response was affected by terrain topography. Only minor differences were detected in reproduction of streamflow between the semi-distributed model and a simple lumped model IHACRES used as a reference. © 2001 Elsevier Science Ltd. All rights reserved.

Keywords: Rainfall-runoff; Modelling; Semi-distributed; Snowmelt; Topography

1. Introduction

Construction and application of mathematical models relating meteorological forcing to the flow measured in the stream has been a major focus of surface water hydrology for decades. A plethora of models, which vary greatly in complexity, have been proposed in the literature to accomplish this task. According to Beck (1991), rainfall-runoff models may loosely be classified into three generic model types, which are (1) metric, (2) conceptual, and (3) physics-based.

Metric models (e.g. Wood and O'Connell, 1985) are strongly observation oriented seeking to characterise system response by extracting information from the existing data, with little or no consideration of the structure of the hydrological system. The idea behind conceptual models (e.g. Franchini and Pacciani, 1991) is to describe all the hydrological processes, which are perceived to be of importance, as simplified conceptualisations. This usually leads to a system of interconnected stores, which are recharged and depleted by appropriate fluxes of the hydrological cycle. Physics-based models (e.g. Abbott et al., 1986) rely on concepts of classical continuum mechanics. The governing partial differential equations can be solved numerically by applying finite difference or finite element computation schemes.

Traditionally rainfall-runoff models have often been applied to problems related to water quantities only, such as real-time flood forecasting, and assessment of the sufficiency of natural water resources. But increasingly, outputs of such models are used to investigate wider environmental problems. These include water quality issues (e.g. Christophersen and Wright, 1981; Cosby et al., 1985), ecological and biological relations in the water environment, and implementation of land-surface schemes for climate models (e.g. Kuhl and Miller, 1992; Leung et al., 1996).

Complex problems call for hydrological models, which can make a distinction between different water

* Corresponding author. Tel. +358-9-451-3831; fax: +358-9-451-3836.

E-mail address: tkokko@water.hut.fi (T. Kokkonen).

1364-8152/01/$ - see front matter
PII: S1364-8152(01)00028-7

transport mechanisms within a catchment, and which can account for spatial variability of terrain properties in the area of interest. Incorporation of detailed process descriptions in the model structure, and allowance for spatial variability of landscape and land use characteristics, easily result in overwhelming data requirements and poorly identifiable model parameters (Beven, 1989; Grayson et al., 1992). In the literature semi-distributed approaches to hydrological modelling have been proposed for circumventing these problems. In TOPMODEL (Beven and Kirkby, 1979; Beven et al., 1994) topography is assumed to be of importance with respect to the hydrological behaviour of a catchment. A topographic index curve, which is derived from a digital elevation model, is used to determine the spatial variability of saturated areas at a given time. Becker (1992) and Becker and Braun (1999) acknowledge the mosaic structure of landscape by aggregating areas of similar hydrological properties into a single 'hydrotope'. Each of these hydrotopes is assigned with its own water balance computation scheme. This kind of a semi-distributed approach cuts down computational demands and the number of model parameters when simulations of streamflow are performed in large catchments (Flügel, 1995).

The semi-distributed approach presented here has been reported earlier in Karvonen et al. (1999), and it rests on the same ideas as those of Becker (1992). Modelling is based on subdivision of a catchment into hydrologically similar areas, which are identified using spatial data on terrain properties. The water balance in each area is calculated using a characteristic profile model (CPM), which relies on a physically consistent description of water movement along a typical travel path from a water divide to the ditch. Discharges from the hydrologically similar areas are combined with the aid of a routing procedure to yield the total streamflow at the catchment outlet.

The objectives of this paper are (1) to demonstrate how differences in terrain properties can be taken into account in the current modelling framework, and (2) to test how well the model simulates streamflow with little calibration. In the small (0.18 km^2) forested catchment studied here the spatial variability in runoff generation is assumed to be dominated by differences in topography. Following this assumption, identification of hydrologically similar areas is solely based on topography. Also, the surface geometry of the typical travel path required in the CPM is determined for each area using the topographical information. The differences of runoff generation in the CPMs are investigated and discussed. In this study an attempt is made to restrict the amount of parameters to be calibrated to the minimum. Whenever possible, parameter values are adopted from existing field measurements or from literature. The modelling scheme used here consists of submodels for snow accumulation and melt, hillslope scale water balance, and channel routing. One parameter of the snow model and the single parameter of the channel routing procedure are calibrated against snow water equivalent and streamflow, respectively. In addition, potential transpiration is scaled by comparison of long-term sums of measured and modelled streamflow. The quality of streamflow reproduction is compared against measured hourly data, and against the results of a simple lumped rainfall-runoff model IHACRES (Jakeman and Hornberger, 1993; Ye et al., 1997).

2. Site description and data

Snow, streamflow and meteorological measurements were carried out during 1997–99 in a forested catchment (Rudbäck, 0.18 km^2) and in an adjacent clear-cut area (about 0.03 km^2) in Siuntio, southern Finland (Fig. 1). The elevation in the area ranges from 34 to 65 m. A digital elevation model (DEM) with 5×5 m resolution was available for the study area.

The catchment is covered by a mature forest stand dominated by Norway spruce. The clearing has a few pine trees left for seeding and small spruces planted after the logging. Bedrock is exposed on the hilltops and soils are composed of silty and sandy moraines with an average depth of 1–2 m to the bedrock. More details on the site are published in Lepistö (1994) and Lepistö and Kivinen (1997).

The climate is temperate with cold, wet winters and precipitation is typically of a relatively low intensity including annually approximately 30% snowfall. Mean annual precipitation, uncorrected for wind effects, during 1991–96 was 700 mm.

A total of 22 snow sticks were placed in the forest to manually measure snow depth on the ground. Water equivalent of snow was measured at three points. Micrometeorological variables at a height of 2 m above the ground were recorded in the clearing and in the forest below the canopy to provide input for a snow energy balance model. Half-hourly data included air temperature, relative humidity, wind speed, downward and reflected short-wave radiation in both sites, and precipitation in the open. Accumulated throughfall in the forest was measured manually at six points approximately once a week. Downward long-wave radiation was measured in the open until January 1999, and the sensor was moved thereafter to the forest. Additional temperature measurements were recorded at a distance of -0.5+0.5 metres from the soil surface and at a height of 10 m in the forest. Hourly streamflow records were available from February 1998 to April 1999 in the stream draining the study catchment. Streamflow was estimated from water level readings at a V-notch weir constructed at the catchment outlet. In wintertime freezing of water hampered

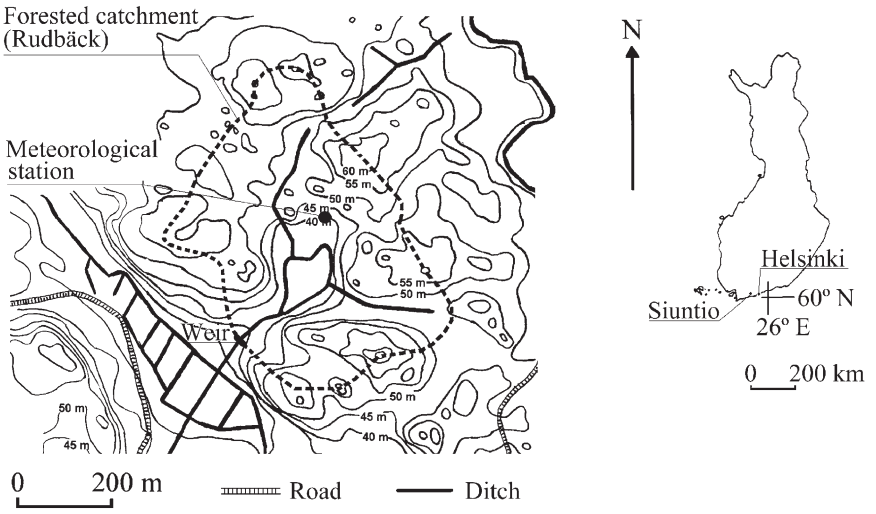

Fig. 1. Location of the Rudbäck catchment in Siuntio. Catchment layout shows the locations of the streamflow measurement weir and the meteorological station in the forest.

the operation of the weir. During field visits ice cover at the weir, when existent, was broken and removed.

The meteorological data were checked and edited to provide continuous hourly input for the hydrological model. Air temperature was compared against manually measured readings to correct for a systematic bias and for large errors during malfunctioning of the measurement system. In February 1999, the air temperature sensor in the forest ceased to operate and the vegetation temperature at a height of 10 m was used instead. Relative humidity was scaled not to exceed 100%. The solar radiation sensors became occasionally covered with snow and the corresponding readings were corrected using the measured upward short-wave radiation and an estimate of the new snow albedo of 0.85. The long-wave radiation measurements were excluded after snowfalls, and the missing values were estimated using the procedure suggested in Satterlund (1979). An estimate of cloudiness was derived from the ratio of the measured short-wave radiation and the simulated clear-sky radiation. For the forested site, a sky-view-fraction of 0.15 was adopted to estimate the contribution of the canopy to the downward long-wave radiation.

Operation of the anemometers was occasionally hampered by intensive snowfalls, and wind speed was not measured in the forest between October 21, 1998 and January 25, 1999. When observed data from one of the two stations (forest and open) were not available, the missing values of wind speed were estimated from the existing records by multiplication with a scaling factor. The factor was selected according to the average ratio (0.21) between the wintertime wind speed in the forest and in the open.

Precipitation in the open was corrected using the procedure recommended for the Finnish H&H measurement gauge in Førland et al. (1996). Six manually operated precipitation gauges in the forest accumulated throughfall between the field visits. The average of the six gauge readings was assumed to represent the cumulative net precipitation in the forest. Stemflow was assumed negligible. Hourly throughfall time-series was derived by scaling the observed hourly precipitation in the open to match the manually measured accumulations in the forest.

3. Methods

3.1. Outline of the semi-distributed hydrological model

Availability of hourly hydrometeorological data from the study catchment enables all components of the hydrological model to operate at an hourly time step. The general principle of the modelling system is shown in Fig. 2. Canopy processes are not modelled but meteorological variables required in the snow model are estimated from measured data. The snow model accounts for accumulation and melt on the ground and gives as an output the discharge out of a melting snowpack. Snowmelt discharge and throughfall together with the potential transpiration form the input for the runoff generation procedure.

In the present study catchment, which has homogeneous land use, topography is assumed to control spatial variability of runoff generation. Typical flowpaths from the catchment boundary to the channel network are extracted from a DEM, and a vertical two-dimensional water balance scheme is applied along each typical path. The water balance scheme is called a characteristic profile model (CPM). The runoff computed in the CPMs is discharged into a routing procedure, which produces

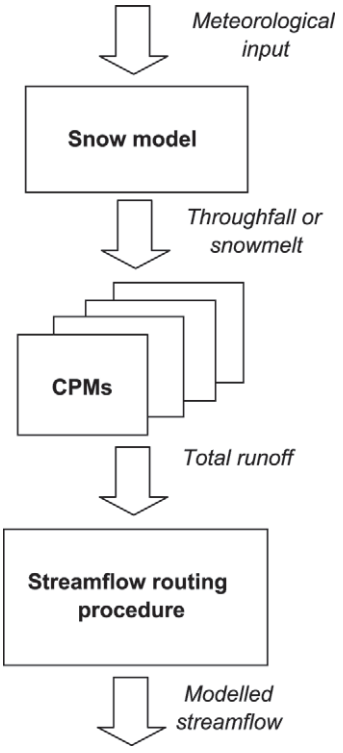

Fig. 2. Schematic representation of the modelling system.

modelled streamflow at the outlet of the catchment. Later in the text, this modelling approach will be referred to as the semi-distributed model.

3.2. Snow model

Snow modelling is based on the energy balance approach as reported in many earlier studies (Anderson, 1976; Morris, 1983; Price and Dunne, 1976; Tarboton et al., 1995). The model simulates net flux of heat through the snowpack into the soil. The procedure is based on the ideas published in Tarboton et al. (1995) and Stähli and Jansson (1998). The snow model uses as input data precipitation/throughfall, net short-wave radiation, downward long-wave radiation, air temperature, relative humidity, and wind speed measured at a height of 2 m above the ground.

In the model there are separate layers for snow and soil. The water equivalent of snow and temperatures at the snow surface, at the soil surface, and in the soil layer are updated at each computation time step.

The heat content of the soil layer, U_g, is given by (e.g. Karvonen, 1988)

$$U_g=(1-\phi)D_g\rho_gC_gT_g+wD_g\rho_wC_wT_g+ID_g\rho_iC_iT_g \quad (1)$$
$$-ID_g\rho_ih_f$$

and

$$w=(w+I)e^{-(T_f-T_g)/d_g} \quad T_g\leq T_f \quad (2)$$

where ϕ is the porosity of the soil, D_g is the thickness of the soil layer, ρ_g is the density of soil grains, C_g is the specific heat of soil, T_g is the average soil temperature, w is the unfrozen water content, ρ_w is the density of water, C_w is the specific heat of water, I is the ice content, ρ_i is the density of ice, C_i is the specific heat of ice, h_f is the latent heat of fusion, T_f is the freezing point temperature, and d_g is a model parameter. The total water content ($w+I$) of the soil was assumed constant. Eq. (2) gives the form of the freezing depression curve, which determines the relationship between the temperature and the unfrozen water content of the soil layer. From Eqs. (1) and (2) the soil layer temperature can be solved iteratively when the heat content of the soil layer is known.

The temperature at the soil surface is computed by assuming a steady-state heat flux from the snow surface through the snowpack into the soil layer (Stähli and Jansson, 1998). According to the steady-state assumption, the heat conduction between snow and soil surfaces is equal to the conduction into the soil layer. This can be formulated as

$$T_{gs}=\frac{T_g+aT_{ss}}{1+a} \quad (3)$$

and

$$a=\frac{k_s\frac{D_g}{2}}{k_gD_s} \quad (4)$$

where T_{gs} is the soil surface temperature, T_{ss} is the snow surface temperature, k_s is the thermal conductivity of snow, k_g is the thermal conductivity of soil, and D_s is the thickness of the snow layer. The thermal conductivity of snow is calculated as a function of snow density according to Anderson (1976), and the thermal conductivity of soil is assumed to be constant.

The net energy flux at the snow surface is split into two terms: heat conducted through the snow, Q_s, and energy M_s that causes snow to melt or is released when liquid water refreezes. These are computed from

$$M_s+Q_s=R_n+H+LE+P \quad (5)$$

where R_n is the net all-wave radiation, H is the sensible heat flux, LE is the latent heat flux, and P is the advective heat flux from precipitation. Positive energy flux is directed downwards. The temperature dependencies are not shown in (5), but it should be noted that all terms except for P are functions of the snow surface temperature (see e.g. Koivusalo et al., 2000; Tarboton et al., 1995). The snow surface temperature is iterated by balancing the atmospheric energy fluxes with the heat conduction into the snowpack. If the iteration results in a temperature greater than 0°C then the temperature is set to 0°C and the excess energy, M_s, causes snow to melt. The snow surface temperature is not allowed to fall

below 0°C as long as there is liquid water in the snowpack. Instead, the net energy flux at the snow surface results in refreezing. A schematic of the snow energy balance computation procedure is shown in Fig. 3.

Sensible and latent heat fluxes are proportional to temperature and vapour pressure gradients, respectively, between the snow surface and a reference height (Tarboton et al., 1995). Turbulent transfer coefficients are computed assuming a logarithmic wind profile above the roughness height of the snow surface. In the present study the roughness height is adjusted by comparing calculated and measured water equivalents of snow. The turbulent transfer coefficients are corrected for atmospheric stability following the method suggested in Price and Dunne (1976). The correction was restricted with a weighting coefficient (see Koivusalo and Heikinheimo, 1999).

The snow melt, L, which is given by

$$L=\frac{M_s}{h_f\rho_w} \tag{6}$$

increases the liquid water content of the snowpack. When the liquid water retention capacity of snow is exceeded, water is discharged out of the snowpack. This discharge is the input for the CPM. Note that in the snow model the total water content of the soil layer is assumed to be constant, i.e. the soil moistures computed in the CPM are not used in the snow model.

3.3. Runoff generation model

3.3.1. Identification of typical flowpaths

Identification of topographical similarity is based on following the path of a water droplet from the water divide to the nearest ditch. All flowpaths starting from the catchment boundary and ending in a ditch are computed. In other words, flowpaths from each grid cell lying at the catchment boundary are followed until they reach a ditch. After the flowpaths have been constructed, the elevation above the ditch as a function of the distance from the ditch is plotted for each flowpath. By looking at these longitudinal sections the flowpaths are categorised according to their length and shape, and typical hillslopes are identified. The share of the catchment area possessing surface topography similar to a typical hillslope is estimated from the number of individual flowpaths belonging to the corresponding category. These typical hillslopes are called *characteristic profiles* (Fig. 4), and for each profile a CPM is constructed. The CPMs describe runoff generation within a catchment. Note that the three-dimensional representation of the elevation surface is thus reduced to a set of typical two-dimensional profiles.

3.3.2. Characteristic profile model (CPM)

The CPM describes soil water movement and runoff generation processes in a characteristic profile, which begins at a water divide and ends in a ditch (Fig. 4). For construction of the CPMs information on surface and bedrock topographies and hydraulic properties of soils are required.

The CPM is a quasi-two-dimensional model in the sense that vertical and lateral water fluxes are computed separately. Lateral flow is assumed to take place only in the saturated zone. The characteristic profile is divided into vertical soil columns, and for each column vertical water fluxes are computed from the Richards equation (Richards, 1931) describing unsaturated–saturated flow in the soil–root system. The Richards equation reads

$$C(h)\frac{\partial h}{\partial t}=\frac{\partial}{\partial z}\left(K_z(h)\frac{\partial h}{\partial z}\right)-\frac{\partial K_z(h)}{\partial z}-S(h)-Q(h) \tag{7}$$

where h is the soil water potential, $K_z(h)$ is the soil hydraulic conductivity, z is the distance from the surface, t is the time, $C(h)$ is the differential water capacity, $S(h)$ accounts for the transpiration in the root zone, and $Q(h)$ accounts for the lateral flow in the saturated zone. The computed soil moisture distributions determine the groundwater levels in all columns.

Downslope groundwater movement between vertical soil columns is computed from Darcy's law

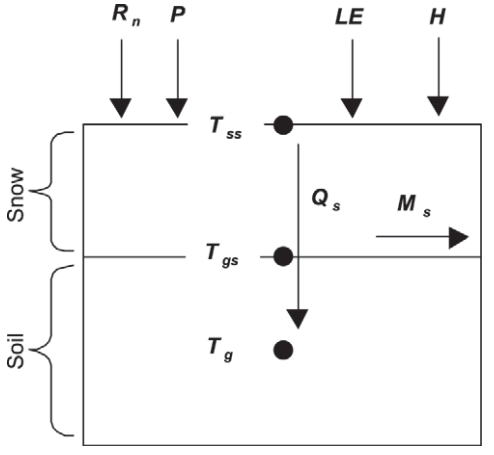

Fig. 3. Illustration of the snow energy balance computation.

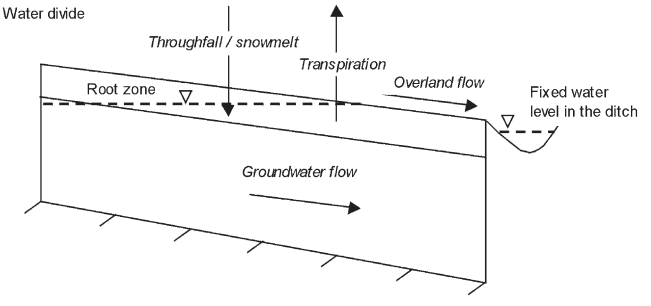

Fig. 4. Schematic representation of a characteristic profile.

$$q_{\mathrm{lat}} = -K_s D \frac{\mathrm{d}H}{\mathrm{d}l} \tag{8}$$

where q_{lat} is the horizontal flow (per unit width) between two columns, K_s is the saturated hydraulic conductivity, D is the thickness of the saturated zone, and $\mathrm{d}H/\mathrm{d}l$ is the groundwater table gradient between the columns. In each column the net groundwater flow, i.e. the difference between flows from an uplsope column to a downslope column, is used to determine $Q(h)$ in Eq. (7) as the volume of water added to the column per unit volume, and per unit time.

The upslope end of a characteristic profile lies at a water divide, and it is assigned with a no-flow boundary condition in the horizontal direction. The boundary condition at the downslope end of the profile is of a fixed head type, and it determines the water level in the ditch. Water flow from the soil profile into the ditch gives the slow response or the base flow component of the total runoff. Flow from the ditch into the soil profile is not allowed. At the bottom of the profile there is a no-flow boundary at the interface between the soil and the impermeable bedrock.

Interception in the understorey vegetation and evaporation from the soil surface are not accounted for, and evapotranspiration is thought to be composed of two components: interception in the overstorey and transpiration. Transpiration E_{at} is controlled by the soil moisture according to the following linear relation given in Feddes et al. (1978)

$$E_{\mathrm{at}} = \begin{cases} E_{\mathrm{pt}}, & h \geq h_{\mathrm{r}} \\ E_{\mathrm{pt}}(h-h_{\mathrm{w}})/(h_{\mathrm{r}}-h_{\mathrm{w}}), & h_{\mathrm{r}} > h \geq h_{\mathrm{w}} \\ 0, & h < h_{\mathrm{w}} \end{cases} \tag{9}$$

where E_{pt} is the potential transpiration, h_{r} is the head at which the soil moisture starts to restrict transpiration, and h_{w} is the wilting point. Potential transpiration is set equal to an estimate of potential evapotranspiration from which interception evaporation has first been subtracted. The depth of water intercepted in the canopy during one time step is estimated as a difference between precipitation in the open and throughfall in the forest, and a running estimate of the depth of water retained in the canopy is maintained. Interception evaporation is calculated by depleting this interception store at a rate equal to potential evapotranspiration until it becomes empty.

Throughfall, or snowmelt discharge, penetrates into the soil if the infiltration capacity allows it. The infiltration capacity gives the maximum amount of water that can enter into the soil matrix during one computation time step. The model generates infiltration excess overland flow (Horton, 1933), if rainfall or snowmelt intensity exceeds the infiltration capacity. Saturation of the entire soil column results in generation of saturation excess overland flow (Dunne and Black, 1970). Surface runoff is routed along the hillslope using the kinematic wave approximation of the St. Venant equations. The implementation is identical to the overland flow computation scheme of the SHE model (Abbott et al., 1986), except that the present model operates in one dimension only.

3.4. Channel network model

According to Kirkby (1993), the delay from rainfall/snowmelt to basin outflow is in small catchments mainly due to hillslope flow processes, but in catchments larger than about 50 km^2 travel times through the channel network generally become increasingly important and ultimately dominate the shape of the hydrograph. Therefore, very simple streamflow routing procedures may be applicable in small catchments. In the present paper, where the study catchment is only 0.18 km^2, a single linear store is used to route water through the channel network. Other model structures, such as the geomorphologic instantaneous unit hydrograph (Rodríguez-Iturbe and Valdés, 1979) have been used previously for this purpose (see e.g. Karvonen et al., 1999). Unlike in the CPM, no physical analogy to real processes is sought after in the structure of the routing procedure.

A CPM yields runoff as water volume per unit area in unit time. The contribution from each CPM to the total runoff is determined by multiplying this runoff with the relative share of the catchment area that the corresponding characteristic profile is assumed to represent. The total runoff is the input to the streamflow routing model.

3.5. IHACRES

IHACRES (Jakeman and Hornberger, 1993; Jakeman et al., 1990; Ye et al., 1997) is a lumped rainfall-runoff model which consists of two modules. The nonlinear rainfall loss module converts rainfall to rainfall excess or effective rainfall, which is defined to be the share of rainfall that eventually becomes streamflow. The linear module represents the transformation of rainfall excess to streamflow.

In the present study the input to IHACRES consists of throughfall in times of no snow, snowmelt discharge in the winter, and potential transpiration. These hourly data are identical to those used as an input to the semi-distributed model.

The nonlinear module utilized in this paper computes the effective rainfall u_k at time step k from

$$u_k = s_k^p r_k \tag{10}$$

where r_k is the throughfall/snowmelt discharge, s_k is the catchment wetness index, and p is a model parameter. The index s_k is calculated by a weighting of the rainfall time series, the weights decaying exponentially backward in time, namely

$$s_k = cr_k + \left(1 - \frac{1}{\tau_w^k}\right) s_{k-1} \quad (11)$$

In Eq. (11) τ_w^k is approximately the time constant, or inversely, the rate at which the catchment wetness declines in the absence of rainfall. The parameter c represents the increase in the wetness index per unit rainfall in the absence of transpiration. It is chosen so that the volume of effective rainfall is equal to the total streamflow volume over the calibration period. To account for seasonal and diurnal fluctuations in the rate at which the catchment dries, the time constant τ_w^k is determined as a function of potential transpiration E_{pt}^k

$$\tau_w^k(E_{pt}^k) = \tau_{w0} \exp[(c_b - E_{pt}^k) f] \quad (12)$$

where f is a modulation parameter on the rate of transpiration, and c_b is an arbitrary constant at which value $\tau_w^k(c_b) = \tau_{w0}$, and τ_{w0} is a model parameter. The structure of the nonlinear module is a simplification of the model presented in Ye et al. (1997).

The linear module of IHACRES allows for a flexible configuration of linear stores connected in parallel and/or series. In this study the linear module consisted of a single linear store, which is fully described by one parameter, namely the time constant τ_l governing the rate of recession in the store.

IHACRES is a parsimonious model having only five calibration parameters in the form applied in the current paper. These are: p, c, τ_{w0}, f, and τ_l.

4. Results and discussion

4.1. Snow model

Hourly meteorological variables required in the snow model were estimated from data measured in the forest below the canopy. All meteorological input variables, and hence the calculated snow water equivalent, were assumed to be spatially uniform within the catchment. The snow model was not calibrated against streamflow but against measured mean water equivalent of snow by adjusting the roughness height of the snow surface. The rest of the snow parameters were fixed a priori, most of them as suggested in Tarboton and Luce (1996).

The calculated water equivalent of snow and the measured mean, minimum and maximum values are presented in Fig. 5 for two winters possessing different characteristics. The winter 1997–1998 was relatively warm and wet with multiple periods of snowmelt throughout the winter. As contrast, there were only few warm spells in the middle of the winter 1998–1999, and significantly higher readings of snow water equivalent were recorded. The spatial variability of the snow water equivalent was high as indicated by the wide range between the measured minimum and maximum values. This variability is a result of spatial differences in throughfall, snow drift, and snowmelt. The model reproduced weekly pattern of the mean snow water equivalent well. Close examination of the snow water equivalent time series at the end of April 1999 reveals that calculated snowmelt commenced slightly later and snow disappeared earlier than the measured mean values suggested. Such fine scale discrepancies are important when snow model output is used to predict hourly streamflows. Weekly measurements did not provide basis for validation of the hourly snowmelt dynamics.

Precipitation in the open and throughfall below the forest canopy are shown in Fig. 6. For winter months, from November to April, interception loss was on the average 23% of the precipitation in the open.

4.2. Construction of CPMs

Recall that in the present study construction of the CPMs is based on following flowpaths from a water divide into a ditch. Meaningful derivation of the flowpaths requires that the channel network mask is consistent with the DEM. To ensure this, the channel network was constructed by adjusting mapped locations of ditches according to drainage accumulation information derived from the DEM. Flow directions were computed according to the Rho8 method of Fairfield and Leymarie (1991). Each grid cell was assigned with a pointer to the receiving cell according to the local aspect, which had been estimated using elevations of all eight neigbouring cells. The pointer was selected stochastically in such a manner that the expected value of the flow direction equalled the local aspect. Subsequently, the directions were modified to ensure flowpath continuity across depressions. Some of the flowpaths are presented in Fig. 7.

Fig. 8 shows the longitudinal sections for all computed flowpaths, i.e. the elevation above ditch level as a function of distance along the flowpath. The elevation was extracted from a DEM that was not adjusted for pits, which explains why elevation along the flowpaths did not always constantly increase from the ditch towards the water divide. For a small portion of the catchment flowpaths were not computed due to data problems in the DEM. Three distinct groups were identified by examining the longitudinal sections. A fourth group was formed from short flowpaths less than 60 m in length. Within each group an average longitudinal section was calculated to represent the entire group. These four aver-

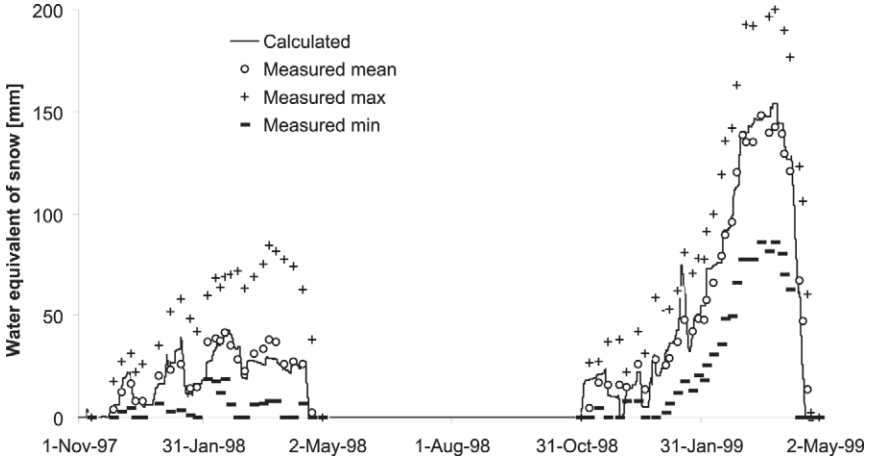

Fig. 5. The calculated water equivalent of snow and the measured mean, minimum and maximum values for two winters (1997–1999).

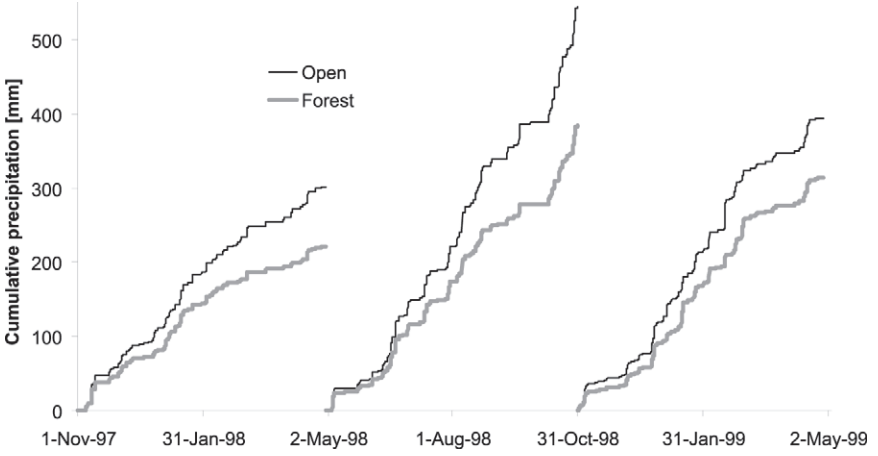

Fig. 6. Cumulative precipitation in the open and below the forest canopy for two winter periods and for one summer period.

age sections determined the length and surface topography of the characteristic profiles. The elevation along characteristic profiles was not allowed to decrease towards the water divide. The relative share of the catchment area that a characteristic profile was assumed to represent was obtained by comparing the number of flowpaths belonging to each group (Fig. 8).

Depth to the bedrock was set to a small value of 0.1 m in the upper 40% of the profiles, which reflects the share of exposed bedrock in the area (41%) as reported in Lepistö and Kivinen (1997). To the lower 60% a value of 1.5 m was given. The longitudinal sections of all four characteristic profiles are plotted in Fig. 9.

Other CPM parameters were the same for all characteristic profiles, and they were also fixed a priori. The value of saturated hydraulic conductivity (0.62 m/d) was based on the results reported in Jauhiainen and Nissinen (1994). Soil water retention characteristics had been measured from soil samples taken at an experimental hillslope lying next to the study catchment (Jauhiainen and Nissinen, 1994, unpublished data), and water retention curves were selected to reflect those measurements. The root depth was set to 0.4 m in columns where the soil depth was 1.5 m, and to 0.1 m elsewhere. Manning coefficient was taken as 0.2 s $m^{-1/3}$. The water level in the ditch was assigned with a constant value of 0.1 m below the surface elevation at the ditch end of the profile.

4.3. Runoff

The model was applied to a period from June 1, 1998 to April 25, 1999. The CPMs required as input time-series of throughfall/snowmelt discharge and potential transpiration. The potential transpiration was assumed to be negligible whenever there was snow on the ground, at other times it was equal to the difference between potential evapotranspiration and interception. The potential evapotranspiration was estimated from the global radiation using the empirical Makkink relationship (Aslyng and Hansen, 1982) with the addition that the estimate was modified in cold temperatures as follows. When the air temperature was below 10°C but above 0°C the estimate was scaled down as a linear function

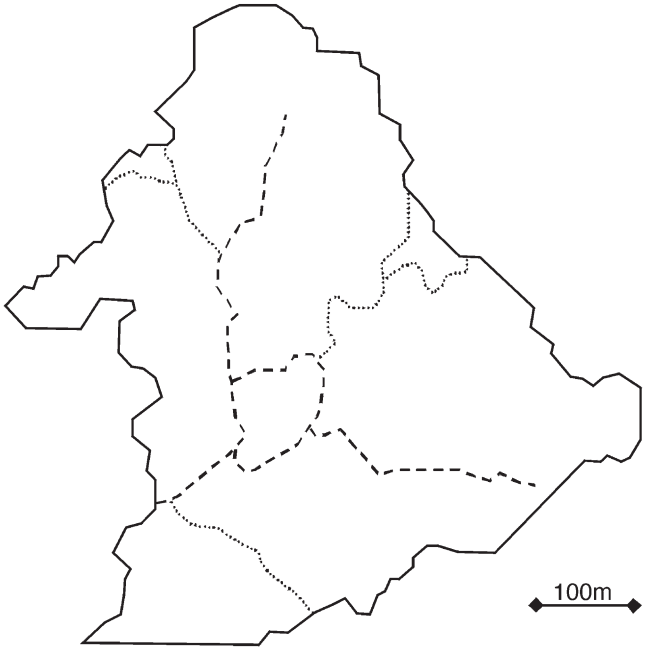

Fig. 7. Catchment border (solid line), channel network (dashed line), and some flowpaths from the water divide into a ditch (dotted lines).

of the temperature, and the potential evapotranspiration was assumed to be equal to zero below 0°C. Finally, the potential transpiration was adjusted by comparison of long-term sums of measured and modelled streamflow.

The channel network submodel, i.e. the time constant of the linear store, was calibrated against hourly data from June 1, 1998 to November 7, 1998. The remaining data were used to test model performance outside the calibration period. Time series of observed and computed streamflows along with the modelling error are graphed for calibration and validation periods in Fig. 10.

Calibration was performed for a time period when there was no snow present and thence the uncertainties inherent in the snow model did not affect stramflow modelling results. In winter, when snow processes had to be simulated, peak flows were often overpredicted giving rise to significanlty poorer fits in the validation period. Cumulative measured and calculated streamflows for the validation period were 273 and 293 mm, respectively. This difference (7%) is relatively small suggesting that the total volume of streamflow was adequately reproduced. As there is hardly any transpiration in the winter, the total computed snowmelt discharge for the same period (300 mm) is also likely to be correct. The less satisfactory streamflow reproduction in the validation period was due to inaccuracies in the representation of snowmelt timing.

The modelling results were compared against the performance of a simple-structured lumped rainfall-runoff model IHACRES, which was driven with the same throughfall, snowmelt discharge, and potential transpiration time series that were used to drive the semi-distributed model. Table 1 gives the efficiencies (Nash and Sutcliffe, 1970) for both models for calibration and validation periods. The two models had only little difference in their performances during the calibration period. The efficiency in the validation was slightly inferior for IHACRES (0.56), resulting mainly from larger streamflow overprediction during spring snowmelt, than for the semi-distributed model (0.61). The difference between the calculated streamflows yielded by the two models is presented in Fig. 10.

Finally, it was examined how different the four characteristic profiles were in their responses to climatic forcing. The approach taken was to compare the cumulative values and temporal variations of runoff from all four profiles. If the differences in runoff values as yielded from the different profiles are insignificant, modelling of the total runoff with several CPMs is not justifiable. Table 2 presents cumulative runoff and its compo-

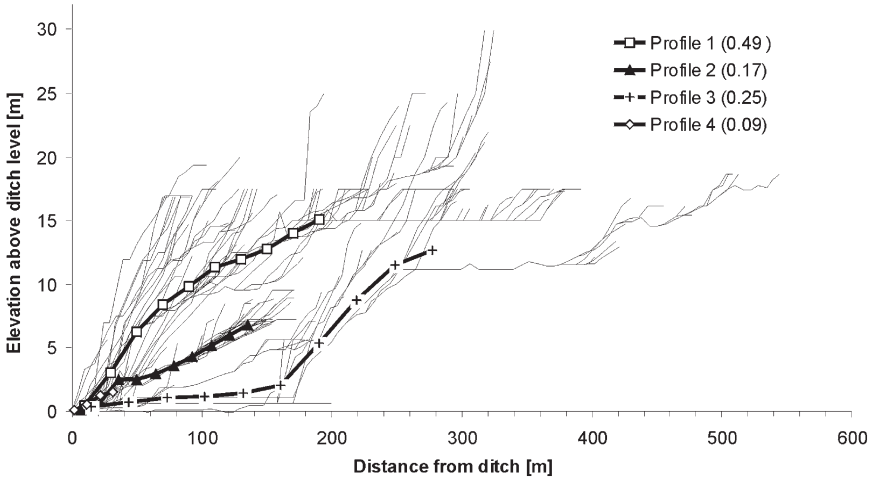

Fig. 8. Surface topography for all computed flowpaths (thin lines). Typical flowpaths are shown as thick lines, and their relative shares are given in parentheses.

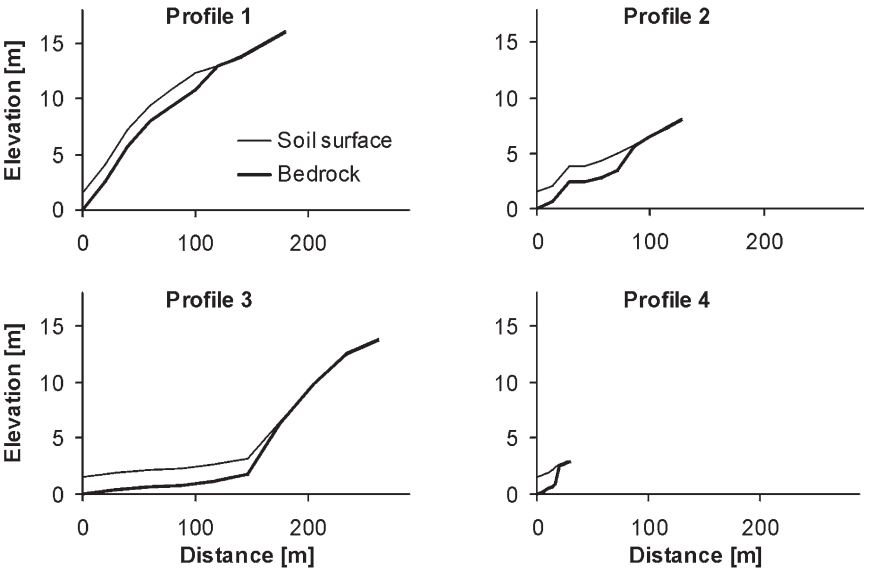

Fig. 9. Longitudinal sections of all four characteristic profiles.

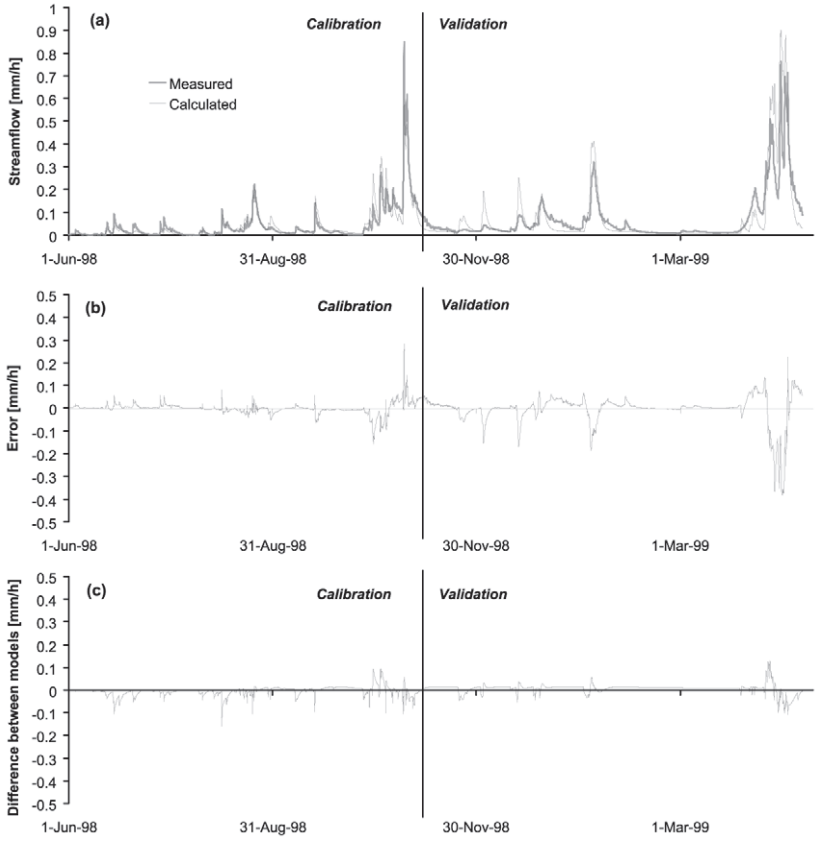

Fig. 10. Measured streamflow and computed streamflow from the semi-distributed model (a), difference between measured streamflow and computed streamflow from the semi-distributed model (b), and difference between computed streamflow from the semi-distributed model and IHACRES (c).

nents for a time period from June 1, 1998, to April 25, 1999. All profiles produced nearly equal amounts of runoff. From Fig. 11, which shows runoff from each profile for spring 1999, it is clear that profile number three produced higher peaks than the others during the first snowmelt events. As the extent of saturation increased with continuing snowmelt the runoff responses of the profiles approached each other. The most apparent difference in

Table 1
Efficiencies in the calibration and validation periods

	Calibration	Validation
Semi-distributed model	0.88	0.61
IHACRES	0.89	0.56

Table 2
Cumulative runoff and its components for a time period from June 1, 1998 to April 25, 1999

	Profile 1	Profile 2	Profile 3	Profile 4
Runoff (mm)	461	466	471	461
Groundwater flow (mm)	13	24	5	159
Overland flow (mm)	448	442	466	302

runoff components was the larger share of groundwater flow from profile number four when compared to others, which is mainly due to the short length of the profile. Due to identical boundary conditions, the maximum volume of groundwater flow is equal for all profiles and hence the groundwater flow (in depth of water) tends to become greater for the short profile. The cumulative runoff components were close to each other for the other three profiles, whose responses were dominated by saturation excess overland flow. According to the model, in saturated conditions all throughfall generates overland flow, which rapidly reaches the channel network without infiltrating into the soil. This is in contradiction with isotope tracer studies (Lepistö, 1994; Lepistö et al., 1994), which suggested that streamflow from the study catchment is to a large extent composed of pre-event water. The modelled partitioning of total runoff into overland and groundwater flow is sensitive to the parameterisation and the boundary conditions of the CPMs. For example, the fixed head boundary condition at the ditch end of the CPM did not account for seasonal water level variation in the ditch. Sensitivity analysis on how runoff components are controlled by the structure and the parameterisation of the CPM will be a topic of future work.

5. Conclusions

The results of the case study revealed only minor differences in the performance between the two very different modelling approaches. If the only objective is to reproduce a streamflow time series from meteorological data, the simple lumped model may be preferable due to ease of its operation. The motivation behind the more laborious and data intensive semi-distributed modelling approach is to take into account areas of variable characteristics within a catchment. In the small catchment studied here spatial variability only in topography was considered. In larger catchments, which comprise of areas with various land use practises, a set of CPMs can be formed on the basis of both topography and land use distribution. Then, the model framework provides some tools to quantify the effects human activities may have on the hydrological response of a catchment (Karvonen et al., 1999).

The CPM parameters were not calibrated, but they were fixed a priori according to the available information. Only the single parameter of the routing model was systematically calibrated against streamflow data, and potential transpiration was scaled by comparison of long-term sums of measured and modelled streamflow. Yet, the semi-distributed model was capable of reproducing the measured streamflow with a fairly good accuracy. This shows some promise with respect to determining parameter values chiefly from field data and reducing the number of calibration parameters to the minimum. If all parameter values were determined a priori from field surveys, the model could be applied to ungauged

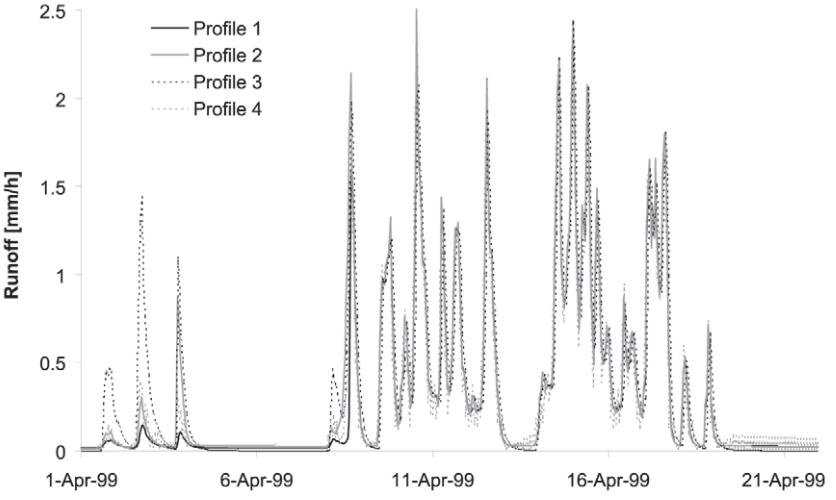

Fig. 11. Runoff from all profiles during springmelt 1999.

catchments where long historical time series of flow data are not available.

Models were calibrated on a snowless period, and then validated to a winter period where performance of both models dropped significantly. The less satisfactory streamflow reproduction in the validation period was due to inaccurate computation of snowmelt timing.

In this study differences in topography were assumed to have a dominant role in explaining spatial variability in runoff generation within a catchment. In terms of cumulative total runoff there were little differences between the four characteristic profiles, but the modelling results suggested that the temporal variability in runoff response was affected by terrain topography.

Future research should be directed towards gaining more appreciation how the semi-distributed modelling framework can be applied to larger catchments. With increasing catchment size the role of stream network becomes more important and hence a single linear store probably is not capable of simulating routing through the network adequately. Also, in a large catchment where the delay in the stream network has a significant role, the distance from the catchment outlet may be of importance. Hence it would be beneficial to consider the locations where the CPMs connect to the stream network. Spatial data on topography, land use, and soils could be used to determine which areas are likely to possess a similar hydrological behaviour.

Acknowledgements

This study was funded by the Academy of Finland project 'Predicting impacts of land use changes on catchment hydrological processess' headed by Professor Pertti Vakkilainen. The authors also received funding from the Land and Water Technology Foundation, and the Finnish Cultural Foundation. The digital elevation model was kindly provided by Dr Ahti Lepistö from the Finnish Environment Institute. Discussions on hydraulic properties of forest soils with Mr Mikko Jauhiainen are acknowledged. Dr Ari Jolma kindly provided the code for flow direction calculations. The reviewers' comments were constructive and improved the manuscript.

References

Abbott, M.B., Bathurst, J.C., Cunge, J.A., O'Connell, P.E., Rasmussen, J.L., 1986. An introduction to the European Hydrology System SHE, 2: structure of a physically-based, distributed modelling system. Journal of Hydrology 87 (1/2), 61–77.

Anderson, E.A., 1976. A point energy and mass balance model of a snow cover. NOAA Technical Report NWS 19.

Aslyng, H.C., Hansen, S., 1982. Water balance and crop production simulation. Model WATCROS for local and regional application. Hydrotechnical Laboratory, The Royal Veterinarian and Agricultural University, Copenhagen.

Beck, M.B., 1991. Forecasting environmental change. Journal of Forecasting 10, 3–19.

Becker, A., 1992. Criteria for a hydrologically sound structuring of large scale land surface process models. In: O'Kane, J.O.P. (Ed.), Advances in Theoretical Hydrology. Elsevier, Amsterdam, pp. 97–111.

Becker, A., Braun, P., 1999. Disaggregation, aggregation and spatial scaling in hydrological modelling. Journal of Hydrology 217 (3–4), 239–252.

Beven, K.J., 1989. Changing ideas in hydrology: the case of physically-based models. Journal of Hydrology 105, 157–172.

Beven, K.J., Kirkby, M.J., 1979. A physically based, variable contributing area model of basin hydrology. Hydrological Sciences Bulletin 24 (1), 43–69.

Beven, K.J., Lamb, R., Quinn, P.F., Romaniwicz, R., Freer, J., 1994. TOPMODEL. In: Singh, V.P. (Ed.), Computer Models of Watershed Hydrology. Water Resources Publications, Highlands Ranch, CO, pp. 627–668.

Christophersen, N., Wright, R.F., 1981. Sulphate budget and a model for sulphate concentrations in stream water at Birkenes, a small forested catchment in southernmost Norway. Water Resources Research 17, 377–389.

Cosby, B.J., Hornberger, G.M., Galloway, J.N., Wright, R.F., 1985. Modelling the effects of acid deposition: assessment of a lumped parameter model of soil water and streamwater chemistry. Water Resources Research 21, 51–63.

Dunne, T., Black, R.D., 1970. Partial area contributions to storm runoff in a small New England watershed. Water Resources Research 6, 1591–1601.

Fairfield, J., Leymarie, P., 1991. Drainage networks from grid digital elevation models. Water Resources Research 27, 709–717.

Feddes, R.A., Kowalik, P.J., Zaradny, H., 1978. Simulation of field water use and crop yield. Centre for Agricultural Publishing and Documentation, Wageningen.

Flügel, W.-A., 1995. Delineating hydrological response units by geographical information system analyses for regional hydrological modelling using PRMS/MMS in the drainage basin of the River Bröl, Germany. Hydrological Processes 9, 423–436.

Førland, E.J., Allerup, P., Dahlström, B., Elomaa, E., Jónsson, T., Madsen, H., Perälä, J., Rissanen, P., Vedin, H., Vejen, F., 1996. Manual for operational correction of nordic precipitation data. DNMI.

Franchini, M., Pacciani, M., 1991. Comparative analysis of several conceptual rainfall-runoff models. Journal of Hydrology 122, 161–219.

Grayson, R.B., Moore, I.D., McMahon, T.A., 1992. Physically based hydrologic modeling, 2, is the concept realistic? Water Resources Research 28, 2659–2666.

Horton, R.E., 1933. The role of infiltration in the hydrological cycle. Transactions, American Geophysical Union 14, 446–460.

Jakeman, A.J., Hornberger, G.M., 1993. How much complexity is warranted in a rainfall-runoff model? Water Resources Research 29, 2637–2649.

Jakeman, A.J., Littlewood, I.G., Whitehead, P.G., 1990. Computation of the instantaneous unit hydrograph and identifiable component flows with application to two small upland catchments. Journal of Hydrology 117, 275–300.

Jauhiainen, M., Nissinen, A., 1994. Calibration of the SOIL model with autumn and summer data of forest soil water tension. In: Kettunen, J., Paasonen-Kivekäs, M., Sirviö, H. (Eds.), Spatial and Temporal Variability and Interdependencies Among Hydrological Processes. Proceedings of a Nordic seminar. NHP, Kirkkonummi, Finland, pp. 17–30.

Karvonen, T., 1988. A model for predicting the effect of drainage on soil moisture, soil temperature and crop yield. Helsinki University of Technology, Espoopp. 215.

Karvonen, T., Koivusalo, H., Jauhiainen, M., Palko, J., Weppling, K., 1999. A hydrological model for predicting runoff from different land use areas. Journal of Hydrology 217 (3–4), 253–265.

Kirkby, M.J., 1993. Network hydrology and geomorphology. In: Beven, K., Kirkby, M.J. (Eds.), Channel Network Hydrology. John Wiley and Sons, Chichester, pp. 1–12.

Koivusalo, H., Heikinheimo, H., 1999. Surface energy exchange over a boreal snowpack: comparison of two snow energy balance models. Hydrological Processes 13 (14–15), 2395–2408.

Koivusalo, H., Heikinheimo, M., Karvonen, T., 2000. Test of a simple two-layer parameterisation to simulate energy balance and temperature of a snowpack. Theoretical and Applied Climatology, accepted for publication.

Kuhl, S.C., Miller, J.R., 1992. Seasonal river runoff calculated from a global atmospheric model. Water Resources Research 28, 2029–2039.

Lepistö, A., 1994. Areas contributing to generation of runoff and nitrate leaching as estimated by empirical isotope methods and TOPMODEL. Aqua Fennica 24, 103–120.

Lepistö, A., Kivinen, Y., 1997. Effects of climatic change on hydrological patterns of a forested catchment: a physically based modeling approach. Boreal Environment Research 2, 19–31.

Lepistö, A., Seuna, P., Bengtsson, L., 1994. The environmental tracer approach in storm runoff studies in forested catchments. In: Seuna, P., Gustard, A., Arnell, N.W., Cole, G.A. (Eds.), FRIEND: Flow Regimes from Experimental and Network Data. Braunschweig Conference. IAHS, pp. 369–379.

Leung, L.R., Wigmosta, M.S., Ghan, S.J., Epstein, D.J., Vail, L.W., 1996. Application of a subgrid orographic precipitation surface hydrology scheme to a mountain watershed. Journal of Geophysical Research—Atmospheres 101 (D8), 12803–12817.

Morris, E.M., 1983. Modelling the flow of mass and energy within a snowpack for hydrological forecasting. Annals of Glaciology 4, 198–203.

Nash, J.E., Sutcliffe, J.V., 1970. River flow forecasting through conceptual models. Part I—a discussion of principles. Journal of Hydrology 10, 282–290.

Price, A.G., Dunne, T., 1976. Energy balance computations of snowmelt in a subarctic area. Water Resources Research 12, 686–694.

Richards, L.A., 1931. Capillary conduction of liquids through porous mediums. Physics 1, 318–333.

Rodríguez-Iturbe, I., Valdés, J., 1979. The geomorphologic structure of hydrologic response. Water Resources Research 15, 1409–1420.

Satterlund, D.R., 1979. An improved equation for estimating longwave radiation from the atmosphere. Water Resources Research 15, 1643–1650.

Stähli, M., Jansson, P.E., 1998. Test of two SVAT snow submodels during different winter conditions. Agricultural and Forest Meteorology 92 (1), 29–41.

Tarboton, D.G., Chowdhury, T.G., Jackson, T.H., 1995. A spatially distributed energy balance snowmelt model. In: Tonnessen, K.A., Williams, M.W., Tranter, M. (Eds.), Biogeochemistry of Seasonally Snow-covered Catchments. IUGG Sumposium, Boulder, July 1995. IAHS, pp. 141–155.

Tarboton, D.G., Luce, C.H., 1996. Utah energy balance snow accumulation and melt model (UEB), computer model technical description and users guide. Utah Water Research Laboratory and USDA Forest Service Intermountain Research Station.

Wood, E.F., O'Connell, P.E., 1985. Real-time forecasting. In: Anderson, M.G., Burt, T.P. (Eds.), Hydrological Forecasting. Wiley, Chichester, pp. 505–558.

Ye, W., Bates, B.C., Viney, N.R., Sivapalan, M., Jakeman, A.J., 1997. Performance of conceptual rainfall-runoff models in low-yielding ephemeral catchments. Water Resources Research 33 (1), 153–166.